


SegHist: A General Segmentation-based Framework for Chinese Historical Document Text Line Detection

Xingjian Hu¹, Baole Wei¹, Liangcai Gao¹(✉), and Jun Wang²

¹ Wangxuan Institute of Computer Technology, Peking University, Beijing, China
{huxingjian, gaoliangcai}@pku.edu.cn

² Department of Information Management, Peking University, Beijing, China

Abstract. Text line detection is a key task in historical document analysis facing many challenges of arbitrary-shaped text lines, dense texts, and text lines with high aspect ratios, etc. In this paper, we propose a general framework for historical document text detection (SegHist), enabling existing segmentation-based text detection methods to effectively address the challenges, especially text lines with high aspect ratios. Integrating the SegHist framework with the commonly used method DB++, we develop DB-SegHist. This approach achieves state-of-the-art (SOTA) on the IACC2022CHDAC (CHDAC), MTHv2, and competitive results on ICDAR2019HDRC Chinese (HDRC) datasets, with a significant improvement of 1.19% on the most challenging CHDAC dataset which features more text lines with high aspect ratios. Moreover, our method attains SOTA on rotated MTHv2 and rotated HDRC, demonstrating its rotational robustness. The code is available at <https://github.com/LumionHXJ/SegHist>.

Keywords: Text line detection · Historical document analysis · Dense Text Detection.

1 Introduction



Fig. 1: Text regions of examples from scene text datasets and historical document datasets. (a) ICDAR2015 [13], (b) SCUT-CTW1500 [46], (c) HDRC [36], (d) CHDAC.

Historical documents analysis [5, 31, 36, 38, 44] is pivotal for preserving and disseminating historical documentary materials. Accurately detecting text line positions is essential for downstream tasks like text recognition and layout understanding. As shown in Fig. 1, compared to texts in natural scenes, texts in

historical documents are denser, and historical documents contain more text lines with high aspect ratios¹. Recent works [12, 15] have improved existing text detection methods to handle arbitrary-shaped text lines in historical documents. However, these methods lack effective improvements for the characteristic of text lines and utilize the rich layout structural information neither.

Segmentation-based methods (*seg-based methods* for short) can represent text lines of arbitrary shapes flexibly, and are highly related to layout segmentation. Unlike regression-based methods (*reg-based methods* for short) that require generating a bounding box for each text line, seg-based methods only need to predict a segmentation map and extract text instances from it, making them suitable for handling numerous text lines in historical documents. Nevertheless, seg-based methods still face difficulties in detecting text in historical documents, particularly in identifying dense texts and text lines with high aspect ratios.

To address these challenges, we extend existing seg-based methods to the historical document environment. We propose a general framework for historical document text detection tasks, named SegHist. SegHist includes the label generation method Text Kernel Stretching (TKS), which can generate segmentation map targets that are easier to learn and predict, targeting the characteristics of text lines in historical document data; the Layout Enhanced Module (LEM) for capturing global information, enhancing the model’s ability to access the rich layout structural information in historical documents; and the Iterative Expansion Distance Post-processor (IEDP), a hyperparameter-free post-processing method that optimizes the shortcomings of low accuracy when directly recovering text regions with high aspect ratios.

The contributions of this paper can be summarized as follows:

1. In response to text lines with high aspect ratios in historical documents, we propose the general seg-based framework SegHist for historical document text detection.
2. We integrate SegHist to DBNet++ [19], resulting in DB-SegHist, which achieves SOTA on the CHDAC, MTHv2, and competitive results on HDRC datasets, with a significant improvement of 1.19% on the most challenging CHDAC datasets, confirming its effectiveness in complex historical documents feature more text lines with high aspect ratios.
3. DB-SegHist attains SOTA on rotated MTHv2 and rotated HDRC datasets, which demonstrating its robustness.

2 Related Work

2.1 Scene Text Detection Methods

Before the era of deep learning, MSER [32] and SWT [9] were mainstream text detection methods that analyzed images by finding correlations in pixel values.

¹ Here, the aspect ratio of a text line refers to the ratio of its longer side to its shorter side. Polygonal text areas, considered as deformed rectangles, have their side lengths calculated through polyline lengths.

In recent years, deep learning methods have achieved good results in scene text detection tasks, surpassing traditional methods. These methods can generally be divided into reg-based methods and seg-based methods.

Regression-Based Methods Reg-based methods approach the problem of text detection as a special case of object detection, obtaining the representation of text instances by directly predicting the control points of bounding boxes. Textboxes [17] applies the SSD [21] framework to text detection by designing anchor boxes with various aspect ratios and incorporating asymmetric convolutional kernels. EAST [48] predicts the quadrangular bounding boxes with high efficiency, enabling accurate detection of inclined text lines. To address the challenge of curved text, ABCNet [22, 24] represents text regions by Bezier curves. Inspired by Mask R-CNN [10], the Mask Textspotter series [16, 30] introduces a mask branch to predict curved text regions more accurately.

However, most of these methods require manual setting of anchors to accommodate the scales and aspect ratios of text lines and a Non-Maximum Suppression (NMS) operation. Drawing on the DETR [2] and Deformable DETR [49], TESTR [47] and DPText-DETR [45] directly predict a specified number of bounding boxes, thereby avoiding these shortcomings. However, they still face difficulties in detecting images with numerous text lines, a common feature in historical document images.

Segmentation-Based Methods Seg-based methods view text detection as a special case of semantic segmentation by predicting whether each pixel belongs to a text region, followed by specific post-processing methods. TextSnake [28] describes text by using a series of discs along the text center line. PSENet [42] utilizes multiple shrinkage levels in prediction and expands text regions during post-processing. PAN [43] additionally predicts a similarity vector, grouping pixels with higher similarity to a text kernel. DB [18] and DB++ [19] simplify the process by introducing differentiable binarization to create a binary map and recover the text instances by unclipping text kernels directly. With their capability to represent texts of arbitrary shapes and effectiveness in handling numerous text lines, seg-based methods are well-suited for historical document text detection.

2.2 Historical Document Text Line Detection Methods

Text detection in historical documents is closely related to scene text detection. Droby et al. [8] demonstrated good adaptability in Arabic historical manuscripts containing various diacritical marks using Mask R-CNN [10]. SeamFormer [39] uses ViT [7] to process historical palm leaf manuscripts in two stages to fit text line polygons. Rahal et al. [34] proposed a lightweight network, L-U-Net, based on FCN [27] for historical document analysis. Although these methods have achieved certain results, their direct application to Chinese historical documents,

which often differ significantly in text line characteristics and layout structure, is challenging.

In the task of text line detection in Chinese historical documents, Ma et al. [31] enhanced the Faster R-CNN framework [35] by adding a character prediction branch, achieving commendable results on the MTHv2 dataset. HisDoc R-CNN [12] applies Mask R-CNN approach [10], employing iterative methods inspired by Cascade R-CNN [1] to refine predictions and accurately detect distorted text lines. DTD [15] integrates the DETR structure [2], adding a mask representation based on discrete Fourier transform, and thus achieves predictions for arbitrarily shaped texts in historical documents. These methods have achieved commendable results, but they lack improvements in the aspect ratio characteristics of text lines and do not fully utilize the layout structure information in historical documents.

3 Methodology

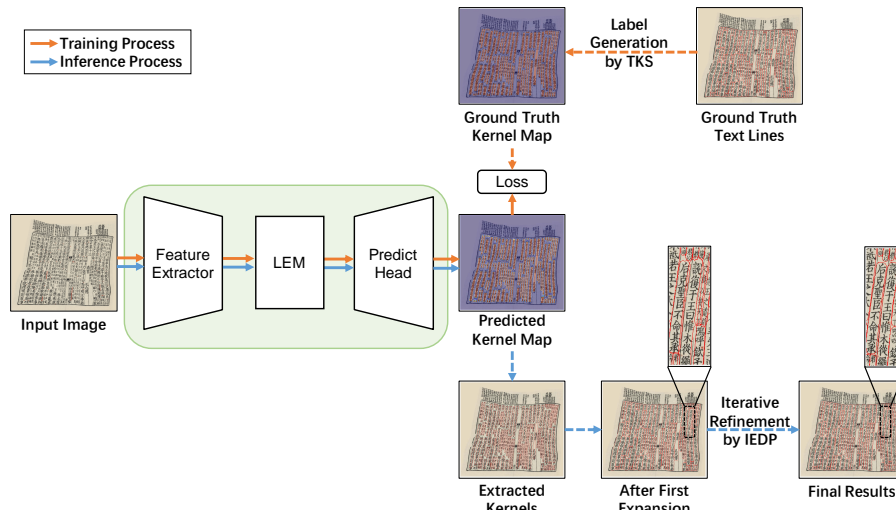


Fig. 2: The pipeline of training and inference process of SegHist. The framework is required to integrate into seg-based methods to achieve a commendable performance, which will be described in Section 3.5.

3.1 Overall Pipeline

To adapt seg-based methods for historical document text detection, we design a general framework, named SegHist. It includes a target generation method (TKS), a global information-capturing module (LEM), and an iterative post-processing method (IEDP). During training, images are passed into a feature extractor that consists of ResNet-50 [11] and Feature Pyramid Network (FPN) [20], followed by a feature fusion module that upsamples the pyramid features. This

process yields features $F \in \mathbb{R}^{C \times H_0 \times W_0}$, where H_0 and W_0 are one quarter of the input image’s height and width, respectively. Features F and learnable layout tokens z are then fed into the LEM and passed to the prediction head to obtain the predicted kernel map. The loss function is computed using this map and the kernel map generated by TKS. During inference, text kernels are extracted from the predicted kernel map and are efficiently and accurately recovered through IEDP. The pipeline of our framework is shown in Fig. 2.

3.2 Text Kernel Stretching

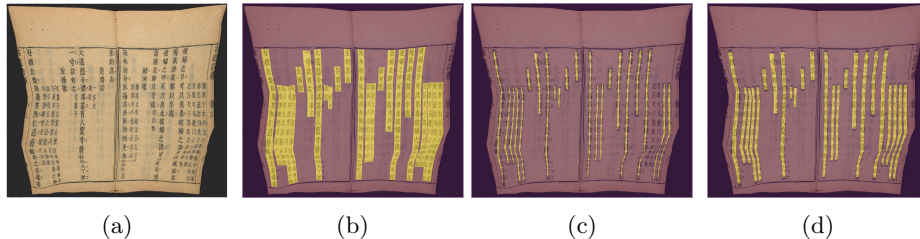


Fig. 3: (a) Historical document from CHDAC dataset. (b) Text region map, suffering from overlapping text instances. (c) Text kernel map generated by DB [18] with default shrink ratio $r = 0.16$, text instances split during shrinkage failed to generate text kernels. (d) Text kernel map generated by TKS ($r = 0, s = 2$).

To avoid the overlap of text instances, seg-based methods commonly separate nearby text instances by predicting the text kernel map. Text kernel is obtained using Vatti clipping algorithm [41], with the shrinkage distance D calculated using text instance’s perimeter L and its area A as follows:

$$D = \frac{A(1-r)}{L}, \quad (1)$$

where r is the shrink ratio.²

The distribution of aspect ratios is depicted in Fig. 4. Text lines in natural scenes tend to have smaller aspect ratios, whereas historical documents display a bimodal distribution, with some instances having higher aspect ratios. In extreme cases, curved instances with high aspect ratios may split into multiple parts, leading to the failure of text kernel generation, as illustrated in Fig. 3c. Furthermore, text lines in historical document images are densely packed, so separating instances with a large r is impractical, presenting a challenge for target generation.

Considering that the text direction in Chinese historical documents is mainly vertical, for simplicity, TKS make the shrinkage along the x-direction only $1/s$ of that along the y-direction, with $s \geq 1$ representing the stretch ratio. By adopting different shrinkage distances for the horizontal and vertical directions in this way,

² In seg-based methods like [18], $D = \frac{A(1-r^2)}{L}$; here, r^2 is replaced with r (where $r < 1$) to achieve a greater shrinking distance.

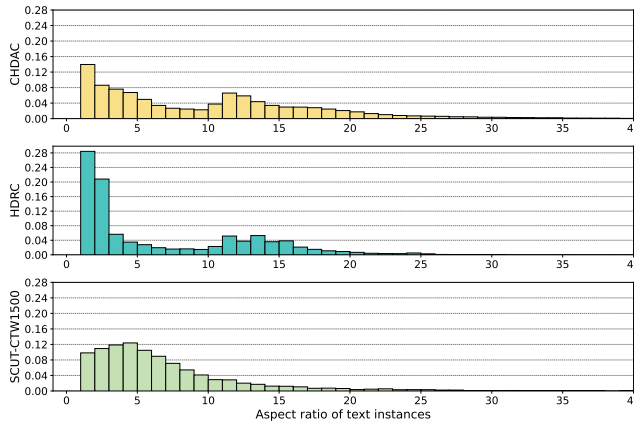


Fig. 4: Aspect ratios distribution of text instances in historical document datasets (CHDAC and HDRC) and in a natural scene dataset (SCUT-CTW1500).

it is possible to separate adjacent text lines while avoiding excessive horizontal shrinkage.

Since seg-based methods predict text kernels, using the post-processing method in DB [18] to recover text regions is a simple and direct approach. Our TKS targets allow for more accurate recovery by this post-processing method. The method employs the Vatti clipping algorithm [41] to expand the predicted kernel, and the expansion distance D' is calculated as follows:

$$D' = \frac{A' \times u}{L'}, \quad (2)$$

where A' and L' are area and perimeter of kernel, respectively, and u is the unclip ratio. Fig. 5 shows the Intersection over Union (IoU) obtained by recovering kernels of vertical text lines with different text aspect ratios³ using different unclip ratios. It is hard to find a universal unclip ratio that accurately recovers kernels with different text aspect ratios generated by DB. However, kernels generated by TKS can be accurately recovered using unclip ratio $u = 1.5$.

3.3 Layout Enhanced Module

To capture the global layout structure without adding excessive parameters and computational load, we design the lightweight LEM. Inspired by MobileFormer [3], LEM consists of multiple Layout Enhanced Blocks (LEB), whose structure is illustrated in Fig. 6. Each LEB takes features $F_{in} \in \mathbb{R}^{C \times H_0 \times W_0}$ and layout tokens $z \in \mathbb{R}^{M \times d}$ as input, and outputs the corresponding F_{out} and z' ,

³ Since TKS treats x-direction and y-direction differently, we use *text aspect ratio* instead of the *aspect ratio* to represent the ratio of the length along the text direction (y-direction for vertical text lines) to the text width (x-direction for vertical text lines). The ratio is computed on text lines rather than kernels.

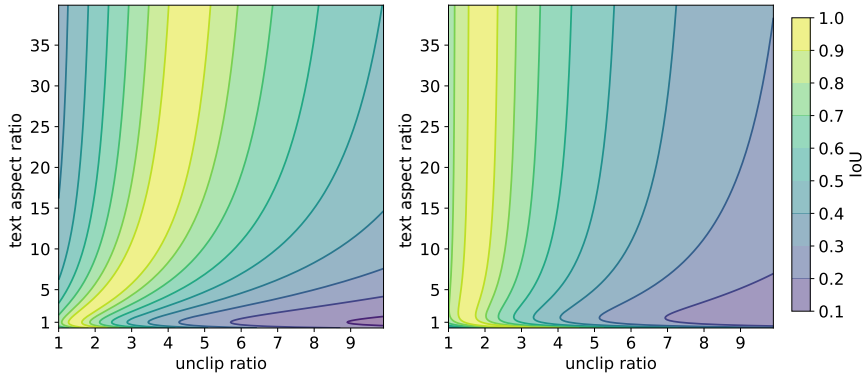


Fig. 5: Recovery IoU of vertical text kernels with different text aspect ratios using different unclip ratios. Left: text kernels generated by DB ($r = 0.16$). Right: text kernels generated by TKS ($r = 0, s = 2$).

each of the same size, respectively. LEB comprises four pillars: Local→Layout, Layout sub-block, Local sub-block, and Local→Layout.

- **Local→Layout.** Local→Layout comprises a multi-head cross-attention and a Feed-Forward Network (FFN) [40]. Considering that the layout often appears as rectangular blocks, we perform both horizontal and vertical max pooling on F_{in} , concatenating to form $\mathbb{R}^{(H_0+W_0) \times C}$, which serves as the keys and values in cross-attention. The layout tokens z act as the queries. To save computation, we only apply a linear transformation to z before calculating the attention.
- **Layout sub-block.** The Layout sub-block adopts the structure of transformer encoder layer [40], resulting in $z' \in \mathbb{R}^{M \times d}$.
- **Local sub-block.** We adopt a bottleneck layer structure [11] in Local sub-block. Specifically, we first reduce channel dimension of F_{in} , obtaining $F_b \in \mathbb{R}^{C_b \times H_0 \times W_0}$. Then, following ConvNext [26], we use a 7×7 convolution with a group width of 4. After each convolution operation, we apply the spatially-aware DY-ReLU [4], the parameters θ_i for pixel i are obtained as follows:

$$\theta_i = \sum_j \alpha_{i,j} f(z'_j), \text{ where } \sum_j \alpha_{i,j} = 1, \quad (3)$$

where α represents the attention between F_b and $z' \cdot W^K$. To save computation, we use the same θ for both DY-ReLU applications.

- **Layout→Local.** Layout→Local includes multi-head cross-attention and a FFN, where attention reuses α computed in the Local sub-block. Lastly, the channels are mapped back to C by a 1×1 convolution.

Due to the decoupling operation in Local→Layout and the introduction of a bottleneck structure, and by largely avoiding direct attention computation on

Based on the above observation, we propose the IEDP. Without significantly increasing the time cost and without introducing hyperparameters, IEDP meets the design requirements of high-precision detectors. The procedure is as follows:

1. Binarize the predicted text kernel map to obtain the binary map.
2. Extract connected components from the binary map to serve as text kernels.
3. For each text kernel, iteratively adjust the expansion distance until the difference between this distance and the newly computed shrinkage distance is sufficiently small. This process is illustrated in Algorithm 1. Note that the expansion along the x-direction is only $1/s$ of that along the y-direction (i.e. **expand in TKS way**).

Algorithm 1 Iterative Expansion

```

1: procedure ITERATIVEEXPANSION(kernel, r, s, tolerance)
2:   Input: kernel - a text kernel represents by a polygon
3:   Input: r, s - the shrink ratio and the stretch ratio used in TKS
4:   Input: tolerance - the tolerance for distance difference
5:    $d \leftarrow \text{INITEXPANSIONDISTANCE}(\textit{kernel}, \textit{r}, \textit{s})$ 
6:    $\textit{step} \leftarrow \textit{distance}/2$ 
7:    $\textit{recovery} \leftarrow \text{EXPANDPOLY}(\textit{kernel}, \textit{d}, \textit{s})$  ▷ Expand in TKS way.
8:    $\textit{d}' \leftarrow \text{GETSHRINKDISTANCE}(\textit{recovery}, \textit{r})$  ▷ Follow Equation (1).
9:   while  $|\textit{d}' - \textit{d}| > \textit{tolerance}$  do
10:    if  $\textit{d}' > \textit{d} + \textit{t}$  then
11:      halve  $\textit{step}$  if it is greater in last iteration
12:       $\textit{d} \leftarrow \textit{d} - \textit{step}$ 
13:    else
14:      halve  $\textit{step}$  if it is less in last iteration
15:       $\textit{d} \leftarrow \textit{d} + \textit{step}$ 
16:    end if
17:     $\textit{recovery} \leftarrow \text{EXPANDPOLY}(\textit{kernel}, \textit{d}, \textit{s})$ 
18:     $\textit{d}' \leftarrow \text{GETSHRINKDISTANCE}(\textit{recovery}, \textit{r})$ 
19:  end while
20: end procedure

```

By properly setting the tolerance in IEDP, the number of iterations can be controlled without significant loss of recovery accuracy, thereby not adding substantial time cost to the post-processing, which will be shown in Section 4.3. As shown in Fig. 7, using IEDP—as opposed to a fixed unclip ratio—can generally achieve a higher level of recovery for text regions with different text aspect ratios, while eliminating the need to adjust the hyperparameters.

3.5 Integrating Framework to Seg-based Methods

As shown in the ablation study of [18], optimizing the text kernel alone often does not yield outstanding results; therefore, SegHist typically needs to be integrated with advanced seg-based methods to achieve better effects. The process of integration with methods (hereinafter referred to as M) includes:

1. Replace objectives of M that involve shrinking or expanding text regions with the objectives generated in TKS way, such as the kernel map and threshold map in DB [18].
2. Insert LEM between the feature extractor and prediction head of M .
3. If the post-processing method of M only uses a single text kernel map (such as DB [18]), use IEDP during inference to recover text regions; otherwise, maintain the original post-processing method (such as progressive scale expansion method of PSENet [42] which uses multiple text kernel maps with different shrinkage distances) to fully utilize the additional prediction targets of M to achieve better results.

By integrating the SegHist framework into existing seg-based methods, our approach transfers the performance of advanced seg-based methods from scene text detection to historical document text line detection.

4 Experiments

4.1 Datasets

CHDAC The dataset⁴ comprises a training set of 2000 images and a test set of 1000 images. In this dataset, regular text lines are represented by quadrilaterals, while distorted text lines are annotated using 16 points. Compared to other historical document datasets, text lines are more densely packed and have larger aspect ratios, presenting a greater challenge.

MTHv2 MTHv2 [31] includes Tripitaka Koreana in Han (TKS) and Multiple Tripitaka in Han (MTH). The training set contains 2399 images, while the test set consists of 800 images. Its text lines are annotated with quadrilaterals.

HDRC HDRC [36] is a collection of Chinese family records images. The training set contains 11,715 images and the test set contains 1,135 images. Text lines are annotated using quadrilaterals. Similar to HisDoc R-CNN [12], we obtained a dataset of 1172 images⁵ and randomly divided it into a training set of 587 images, a validation set of 117 images, and a test set of 468 images.

4.2 Implementation Details

We integrated the SegHist framework to DB++ [19], resulting in DB-SegHist. The DB-SegHist utilized a ResNet-50 [11] pretrained on ImageNet [6] with FPN [20] as backbone. In TKS, we used a shrink ratio $r = 0$ and a stretch

⁴ Official website of the CHDAC competition: <https://iacc.pazhoulab-huangpu.com/>. Similar to HisDoc R-CNN, we only utilized the official dataset and did not use any data submitted by the participants.

⁵ https://tc11.cvc.uab.es/datasets/ICDAR2019HDRC_1

ratio $s = 2$. Three layers of LEB were used to compose the LEM, which utilized 8 learnable layout tokens. During training, we used OHEM [37] to balance positive and negative samples. For evaluation, we employed the IEDP method for post-processing.

Our model was trained on 4 NVIDIA GeForce RTX 2080 Ti GPUs with a batch size of 4, for a total of 30k iterations. We used mixed-precision training [33], optimized with AdamW [29], set the initial learning rate to 1×10^{-4} , weight decay coefficient to 1×10^{-4} , and decayed the learning rate by 0.1 at 50% and 80% of the total iterations. Both our training and testing were based on the MMOCR toolkit [14].

Additionally, we adopted the data augmentation settings from HisDoc R-CNN for training and testing. Our models were trained using color jittering, flipping, rotating, resizing, and cropping as augmentation techniques. Images were resized to (1333, 800) during testing while keeping their ratio. When assessing the model’s robustness to rotated historical document images, we performed random rotations from -15° to 15° on test dataset images from the MTHv2 and the HDRC.

4.3 Ablation Study

Table 1: The ablation results of DB-SegHist on the CHDAC dataset. Here, P_{50} , R_{50} , and F_{50} represent the precision, recall, and F-measure, respectively, at an IoU threshold of 0.5; F_{75} represents the F-measure at an IoU threshold of 0.75. *Time* indicates the average inference time per image on our single GPU setup. All images were resized to (1333, 800) while keeping their ratios.

Baseline	TKS	LEM	IEDP	P_{50}	R_{50}	F_{50}	F_{75}	Time (s)
DB++				92.43	83.89	87.95	64.91	0.0809
			✓	93.68	82.57	87.77	69.05	0.0960
	✓			98.01	94.93	96.45	90.46	0.1082
	✓		✓	97.98	94.90	96.42	91.67	0.1285
	✓	✓		98.39	95.90	97.13	91.80	0.1236
	✓	✓	✓	98.36	95.88	97.11	92.96	0.1394

Effectiveness of TKS When without TKS, we calculated the shrinkage distance using Equation (1), with r set to 0.16. As shown in Table 1, the introduction of TKS results in significant improvements in various metrics for DB++. Specifically, TKS achieves performance gains of 8.50% and 25.55% in terms of F_{50} and F_{75} , respectively. These results indicate that incorporating TKS can effectively adapt to the environment of historical documents.

Effectiveness of LEM In Table 1, when comparing TKS+LEM with TKS, under an IoU threshold of 0.5, the F-score increases by 0.68%, with the recall rate increases by 0.97%. Under an IoU threshold of 0.75, the F-score increases by

1.34%. Furthermore, the total parameters of LEM used in the model is 0.95M, with an additional time overhead of approximately 0.013s per image. These confirm its efficiency in terms of both space and time.

Effectiveness of IEDP Firstly, we tested different unclip ratios on a subset of the training dataset to obtain the average IoU when directly recovering text kernels generated by both the standard DB++ and TKS. Ultimately, we adopted an $u = 2.5$ when using DB++ targets and $u = 1.8$ when using TKS targets. Please note that when recovering TKS kernels with the DB post-processing method, it is required to expand in TKS way.

The results in Table 1 indicate that the use of IEDP does not lead to a significant improvement when the IoU threshold is set to 0.5. However, as the IoU threshold increases, under DB++, TKS, and TKS+LEM, the use of IEDP results in F-score improvements of 4.14%, 1.21%, and 1.16%, respectively. These results confirm the necessity of IEDP for constructing a high-precision text detector. Furthermore, IEDP is more conducive to building a universal historical document text detector because it is parameter-free.

Effectiveness on Different Text Aspect Ratios As shown in Fig. 8, before introducing TKS, the model has low accuracy, and the performance in recovering text lines with high text aspect ratios (e.g. ratios larger than 10) is inferior compared to those with low text aspect ratios (e.g. ratios between 1 and 10). After incorporating TKS, the prediction and recovery of text lines become more accurate, with performance on higher text aspect ratios becoming more stable. Subsequently, using IEDP for post-processing results in more accurate recovery, especially offering a more significant improvement for text lines with high aspect ratios. These results demonstrate that TKS and IEDP significantly enhance the capability to detect text lines in historical documents, especially those with high text aspect ratios.

4.4 Comparison with Previous Methods

In this section, we evaluate the performance of our approach on all three benchmarks. On the CHDAC dataset, we integrated the SegHist framework to PSENet [42] and PAN [43], resulting in PSE-SegHist and PAN-SegHist, respectively. As explained in Section 3.5, while DB-SegHist used IEDP for post-processing, PSE-SegHist and PAN-SegHist retained their original post-processors. Precision, recall, and F-score are all computed at an IoU threshold of 0.5.

Text Detection on Historical Documents The experimental results on the CHDAC, MTHv2, and HDRC datasets are shown in Tables 2 and Table 3. Our method achieves SOTA F-score levels on the CHDAC and MTHv2 datasets under the use of ResNet-50 [11] as the backbone, surpassing the previous SOTA by 1.19% on the CHDAC dataset. The results of PSE-SegHist and PAN-SegHist

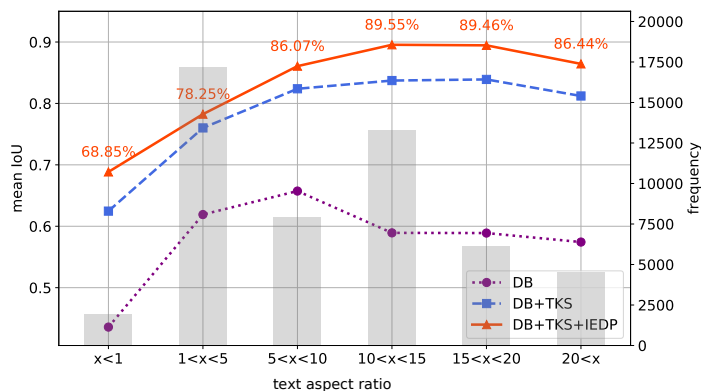


Fig. 8: Average IoU of text lines with different text aspect ratios on the CHDAC. When not using IEDP for post-processing, we adhered to DB’s default settings with $u = 1.5$.

Table 2: Detection results of different methods on CHDAC. This dataset includes curved text lines annotated using 16 points. P , R , and F indicate the precision, recall, and F-measure, respectively, at an IoU threshold of 0.5. **Bold** indicates SOTA and underline indicates the second-best result.

Method	P	R	F
EAST [48]	61.41	73.13	66.76
Mask R-CNN [10]	89.03	80.90	84.77
Cascade R-CNN [1]	92.82	83.63	87.98
OBDD [23]	94.73	81.52	87.63
TextSnake [28]	96.33	89.62	92.85
PSENet [42]	76.99	89.62	82.83
PAN [43]	92.74	85.71	89.09
FCENet [50]	88.42	85.04	86.70
DBNet++ [19]	91.39	89.15	90.26
HisDoc R-CNN [12]	<u>98.19</u>	93.74	95.92
PSE-SegHist(ours)	97.00	<u>95.31</u>	<u>96.15</u>
PAN-SegHist(ours)	97.52	94.77	96.12
DB-SegHist(ours)	98.36	95.88	97.11

Table 3: Detection results of different methods on the MTHv2 dataset and the HDRC dataset at an IoU threshold of 0.5. Text lines in both datasets are annotated by quadrilaterals. * indicates the use of Swin Transformer [25] as backbone, and † indicates the requirement of character annotations.

Method	MTHv2			HDRC		
	P	R	F	P	R	F
EAST [48]	-	-	95.04	83.36	87.70	85.47
Ma et al.† [31]	-	-	97.72	-	-	-
Mask R-CNN [10]	95.83	96.35	96.09	94.50	95.11	94.81
Cascade R-CNN [1]	98.57	96.52	97.53	<u>94.73</u>	<u>95.28</u>	<u>95.00</u>
OBD [23]	98.17	97.19	97.68	94.45	94.78	94.61
TextSnake [28]	94.31	91.77	93.02	81.70	72.95	77.07
PSENet [42]	96.87	95.82	96.34	92.83	93.68	93.25
PAN [43]	97.65	95.28	96.45	93.34	89.34	91.30
FCENet [50]	92.47	88.19	90.28	92.38	91.11	91.74
DBNet++ [19]	93.48	93.22	93.35	93.10	91.05	92.06
HisDoc R-CNN [12]	98.57	97.05	97.80	94.61	95.65	95.13
Deformable DETR* [49]	97.92	94.64	96.25	-	-	-
DTDT* [15]	97.94	97.86	97.90	-	-	-
DB-SegHist(ours)	<u>98.30</u>	<u>97.45</u>	<u>97.87</u>	94.79	94.31	94.55

Table 4: Detection results of different methods on rotated version of MTHv2 and HDRC at an IoU threshold of 0.5.

Method	Rotated MTHv2			Rotated HDRC		
	P	R	F	P	R	F
EAST [48]	87.01	89.61	88.29	87.46	89.02	88.23
Mask R-CNN [10]	44.27	37.65	40.69	37.19	31.25	33.96
Cascade R-CNN [1]	60.63	44.32	51.21	42.73	33.17	37.35
OBD [23]	97.49	84.72	90.66	93.94	88.59	91.18
TextSnake [28]	94.46	88.45	91.36	83.96	69.96	76.32
PSENet [42]	90.16	89.70	89.93	86.67	91.49	89.01
PAN [43]	97.39	91.58	94.40	92.67	84.75	88.53
FCENet [50]	89.96	89.83	89.89	89.35	87.70	88.52
DBNet++ [19]	89.92	90.16	90.04	92.95	90.75	91.84
HisDoc R-CNN [12]	<u>98.21</u>	<u>96.01</u>	<u>97.10</u>	<u>94.36</u>	94.35	<u>94.36</u>
DB-SegHist(ours)	98.38	96.39	97.38	94.60	<u>94.21</u>	94.40

on CHDAC also show the universality of our framework. Since the text regions in the HDRC dataset are not closely aligned with the actual text areas and contain a considerable number of background pixels, it is challenging for seg-based methods to make accurate per-pixel predictions. The performance of existing seg-based methods on this dataset generally fall short of that achieved by reg-based methods. Compared to other seg-based approaches, our method shows significant improvements by achieving an F-score of 94.55%, which is comparable to the SOTA method’s F-score of 95.13%.

Text Detection on Rotated Historical Documents As shown in the Table 4, results on Rotated MTHv2 and Rotated HDRC demonstrate DB-SegHist’s rotational robustness, with F-scores of 97.38% and 94.40%, respectively, both reaching SOTA levels. In comparison, reg-based methods might require angle prediction to achieve rotational robustness, whereas seg-based methods, due to their pixel-level predictions and text kernel extraction through connected components, inherently perform well in detecting rotated texts. Our SegHist framework inherits this advantage, exhibiting excellent rotational robustness.

4.5 Limitation



Fig. 9: Examples where our method fails. Left: ground truth. Right: prediction of DB-SegHist. False negatives are marked in red, false positives are shown in green, and other colors are used to display the correspondence between the text lines of the ground truth and the prediction results.

Although DB-SegHist demonstrates commendable performance in detecting text in historical documents, particularly for text lines with a text aspect ratio greater than 10, its performance in detecting regions with text aspect ratios less

than 5 is still not ideal, as shown in Fig. 8. These regions typically appear as annotations or notes, with smaller sizes and fewer characters. As shown in Fig. 9, although our method is accurate in detecting the main text, it often misses these smaller areas.

Furthermore, since detecting historical documents is closely linked to text recognition, merely considering the F-score of detection is not sufficient. For example, even if a text region is split in prediction, with all characters in the region being detected, it may not result in any loss to the overall Optical Character Recognition (OCR) results, yet it may be considered a complete miss under current metrics. Conversely, for longer text lines, detection may be considered successful even if some characters are missed. The aforementioned phenomenon is not rare and can be observed in Fig. 9. Thus, the performance of detectors should be evaluated based on their ability to assist in text recognition.

5 Conclusion

In this paper, we develop a general framework, SegHist, which extends seg-based methods to historical document data by addressing the challenges of dense texts and text lines with high aspect ratios. Experimental results demonstrate that our DB-SegHist achieves competitive performance across three historical document benchmarks and exhibits strong rotational robustness.

Acknowledgement

This work is supported by the projects of National Science and Technology Major Project (2021ZD0113301) and the National Natural Science Foundation of China (No. 62376012), which is also a research achievement of the Key Laboratory of Science, Technology and Standard in Press Industry (Key Laboratory of Intelligent Press Media Technology).

References

1. Cai, Z., Vasconcelos, N.: Cascade r-cnn: Delving into high quality object detection. In: Proceedings of the IEEE conference on computer vision and pattern recognition. pp. 6154–6162 (2018)
2. Carion, N., Massa, F., Synnaeve, G., Usunier, N., Kirillov, A., Zagoruyko, S.: End-to-end object detection with transformers. In: European conference on computer vision. pp. 213–229. Springer (2020)
3. Chen, Y., Dai, X., Chen, D., Liu, M., Dong, X., Yuan, L., Liu, Z.: Mobile-former: Bridging mobilenet and transformer. In: Proceedings of the IEEE/CVF Conference on Computer Vision and Pattern Recognition. pp. 5270–5279 (2022)
4. Chen, Y., Dai, X., Liu, M., Chen, D., Yuan, L., Liu, Z.: Dynamic relu. In: European Conference on Computer Vision. pp. 351–367. Springer (2020)
5. Cheng, H., Jian, C., Wu, S., Jin, L.: Scut-cab: A new benchmark dataset of ancient chinese books with complex layouts for document layout analysis. In: International Conference on Frontiers in Handwriting Recognition. pp. 436–451. Springer (2022)

6. Deng, J., Dong, W., Socher, R., Li, L.J., Li, K., Fei-Fei, L.: Imagenet: A large-scale hierarchical image database. In: 2009 IEEE conference on computer vision and pattern recognition. pp. 248–255. Ieee (2009)
7. Dosovitskiy, A., Beyer, L., Kolesnikov, A., Weissenborn, D., Zhai, X., Unterthiner, T., Dehghani, M., Minderer, M., Heigold, G., Gelly, S., et al.: An image is worth 16x16 words: Transformers for image recognition at scale. arXiv preprint arXiv:2010.11929 (2020)
8. Drobny, A., Kurar Barakat, B., Alaasam, R., Madi, B., Rabaev, I., El-Sana, J.: Text line extraction in historical documents using mask r-cnn. *Signals* **3**(3), 535–549 (2022)
9. Epshtein, B., Ofek, E., Wexler, Y.: Detecting text in natural scenes with stroke width transform. In: 2010 IEEE computer society conference on computer vision and pattern recognition. pp. 2963–2970. IEEE (2010)
10. He, K., Gkioxari, G., Dollár, P., Girshick, R.: Mask r-cnn. In: Proceedings of the IEEE international conference on computer vision. pp. 2961–2969 (2017)
11. He, K., Zhang, X., Ren, S., Sun, J.: Deep residual learning for image recognition. In: Proceedings of the IEEE conference on computer vision and pattern recognition. pp. 770–778 (2016)
12. Jian, C., Jin, L., Liang, L., Liu, C.: Hisdoc r-cnn: Robust chinese historical document text line detection with dynamic rotational proposal network and iterative attention head. In: International Conference on Document Analysis and Recognition. pp. 428–445. Springer (2023)
13. Karatzas, D., Gomez-Bigorda, L., Nicolaou, A., Ghosh, S., Bagdanov, A., Iwamura, M., Matas, J., Neumann, L., Chandrasekhar, V.R., Lu, S., et al.: Icdar 2015 competition on robust reading. In: 2015 13th international conference on document analysis and recognition (ICDAR). pp. 1156–1160. IEEE (2015)
14. Kuang, Z., Sun, H., Li, Z., Yue, X., Lin, T.H., Chen, J., Wei, H., Zhu, Y., Gao, T., Zhang, W., et al.: Mmocr: A comprehensive toolbox for text detection, recognition and understanding. In: Proceedings of the 29th ACM International Conference on Multimedia. pp. 3791–3794 (2021)
15. Li, H., Liu, C., Wang, J., Huang, M., Zhou, W., Jin, L.: Dtdt: Highly accurate dense text line detection in historical documents via dynamic transformer. In: International Conference on Document Analysis and Recognition. pp. 381–396. Springer (2023)
16. Liao, M., Pang, G., Huang, J., Hassner, T., Bai, X.: Mask textspotter v3: Segmentation proposal network for robust scene text spotting. In: Computer Vision–ECCV 2020: 16th European Conference, Glasgow, UK, August 23–28, 2020, Proceedings, Part XI 16. pp. 706–722. Springer (2020)
17. Liao, M., Shi, B., Bai, X., Wang, X., Liu, W.: Textboxes: A fast text detector with a single deep neural network. In: Proceedings of the AAAI conference on artificial intelligence. vol. 31 (2017)
18. Liao, M., Wan, Z., Yao, C., Chen, K., Bai, X.: Real-time scene text detection with differentiable binarization. In: Proceedings of the AAAI conference on artificial intelligence. vol. 34, pp. 11474–11481 (2020)
19. Liao, M., Zou, Z., Wan, Z., Yao, C., Bai, X.: Real-time scene text detection with differentiable binarization and adaptive scale fusion. *IEEE Transactions on Pattern Analysis and Machine Intelligence* **45**(1), 919–931 (2022)
20. Lin, T.Y., Dollár, P., Girshick, R., He, K., Hariharan, B., Belongie, S.: Feature pyramid networks for object detection. In: Proceedings of the IEEE conference on computer vision and pattern recognition. pp. 2117–2125 (2017)

21. Liu, W., Anguelov, D., Erhan, D., Szegedy, C., Reed, S., Fu, C.Y., Berg, A.C.: Ssd: Single shot multibox detector. In: *Computer Vision–ECCV 2016: 14th European Conference, Amsterdam, The Netherlands, October 11–14, 2016, Proceedings, Part I* 14. pp. 21–37. Springer (2016)
22. Liu, Y., Chen, H., Shen, C., He, T., Jin, L., Wang, L.: Abcnet: Real-time scene text spotting with adaptive bezier-curve network. In: *proceedings of the IEEE/CVF conference on computer vision and pattern recognition*. pp. 9809–9818 (2020)
23. Liu, Y., He, T., Chen, H., Wang, X., Luo, C., Zhang, S., Shen, C., Jin, L.: Exploring the capacity of an orderless box discretization network for multi-orientation scene text detection. *International Journal of Computer Vision* **129**, 1972–1992 (2021)
24. Liu, Y., Shen, C., Jin, L., He, T., Chen, P., Liu, C., Chen, H.: Abcnet v2: Adaptive bezier-curve network for real-time end-to-end text spotting. *IEEE Transactions on Pattern Analysis and Machine Intelligence* **44**(11), 8048–8064 (2021)
25. Liu, Z., Lin, Y., Cao, Y., Hu, H., Wei, Y., Zhang, Z., Lin, S., Guo, B.: Swin transformer: Hierarchical vision transformer using shifted windows. In: *Proceedings of the IEEE/CVF international conference on computer vision*. pp. 10012–10022 (2021)
26. Liu, Z., Mao, H., Wu, C.Y., Feichtenhofer, C., Darrell, T., Xie, S.: A convnet for the 2020s. In: *Proceedings of the IEEE/CVF conference on computer vision and pattern recognition*. pp. 11976–11986 (2022)
27. Long, J., Shelhamer, E., Darrell, T.: Fully convolutional networks for semantic segmentation. In: *Proceedings of the IEEE conference on computer vision and pattern recognition*. pp. 3431–3440 (2015)
28. Long, S., Ruan, J., Zhang, W., He, X., Wu, W., Yao, C.: Textsnake: A flexible representation for detecting text of arbitrary shapes. In: *Proceedings of the European conference on computer vision (ECCV)*. pp. 20–36 (2018)
29. Loshchilov, I., Hutter, F.: Decoupled weight decay regularization. *arXiv preprint arXiv:1711.05101* (2017)
30. Lyu, P., Liao, M., Yao, C., Wu, W., Bai, X.: Mask textspotter: An end-to-end trainable neural network for spotting text with arbitrary shapes. In: *Proceedings of the European conference on computer vision (ECCV)*. pp. 67–83 (2018)
31. Ma, W., Zhang, H., Jin, L., Wu, S., Wang, J., Wang, Y.: Joint layout analysis, character detection and recognition for historical document digitization. In: *2020 17th International Conference on Frontiers in Handwriting Recognition (ICFHR)*. pp. 31–36. IEEE (2020)
32. Matas, J., Chum, O., Urban, M., Pajdla, T.: Robust wide-baseline stereo from maximally stable extremal regions. *Image and vision computing* **22**(10), 761–767 (2004)
33. Micikevicius, P., Narang, S., Alben, J., Diamos, G., Elsen, E., Garcia, D., Ginsburg, B., Houston, M., Kuchaiev, O., Venkatesh, G., et al.: Mixed precision training. *arXiv preprint arXiv:1710.03740* (2017)
34. Rahal, N., Vögtlin, L., Ingold, R.: Layout analysis of historical document images using a light fully convolutional network. In: *International Conference on Document Analysis and Recognition*. pp. 325–341. Springer (2023)
35. Ren, S., He, K., Girshick, R., Sun, J.: Faster r-cnn: Towards real-time object detection with region proposal networks. *Advances in neural information processing systems* **28** (2015)
36. Saini, R., Dobson, D., Morrey, J., Liwicki, M., Liwicki, F.S.: Icdar 2019 historical document reading challenge on large structured chinese family records. In: *2019 International Conference on Document Analysis and Recognition (ICDAR)*. pp. 1499–1504. IEEE (2019)

37. Shrivastava, A., Gupta, A., Girshick, R.: Training region-based object detectors with online hard example mining. In: Proceedings of the IEEE conference on computer vision and pattern recognition. pp. 761–769 (2016)
38. Sihang, W., Jiapeng, W., Weihong, M., Lianwen, J.: Precise detection of chinese characters in historical documents with deep reinforcement learning. *Pattern Recognition* **107**, 107503 (2020)
39. Vadlamudi, N., Krishna, R., Sarvadevabhatla, R.K.: Seamformer: High precision text line segmentation for handwritten documents. In: International Conference on Document Analysis and Recognition. pp. 313–331. Springer (2023)
40. Vaswani, A., Shazeer, N., Parmar, N., Uszkoreit, J., Jones, L., Gomez, A.N., Kaiser, L., Polosukhin, I.: Attention is all you need. *Advances in neural information processing systems* **30** (2017)
41. Vatti, B.R.: A generic solution to polygon clipping. *Communications of the ACM* **35**(7), 56–63 (1992)
42. Wang, W., Xie, E., Li, X., Hou, W., Lu, T., Yu, G., Shao, S.: Shape robust text detection with progressive scale expansion network. In: Proceedings of the IEEE/CVF conference on computer vision and pattern recognition. pp. 9336–9345 (2019)
43. Wang, W., Xie, E., Song, X., Zang, Y., Wang, W., Lu, T., Yu, G., Shen, C.: Efficient and accurate arbitrary-shaped text detection with pixel aggregation network. In: Proceedings of the IEEE/CVF international conference on computer vision. pp. 8440–8449 (2019)
44. Xie, Z., Huang, Y., Jin, L., Liu, Y., Zhu, Y., Gao, L., Zhang, X.: Weakly supervised precise segmentation for historical document images. *Neurocomputing* **350**, 271–281 (2019)
45. Ye, M., Zhang, J., Zhao, S., Liu, J., Du, B., Tao, D.: Dptext-detr: Towards better scene text detection with dynamic points in transformer. In: Proceedings of the AAAI Conference on Artificial Intelligence. vol. 37, pp. 3241–3249 (2023)
46. Yuliang, L., Lianwen, J., Shuaitao, Z., Sheng, Z.: Detecting curve text in the wild: New dataset and new solution. *arXiv preprint arXiv:1712.02170* (2017)
47. Zhang, X., Su, Y., Tripathi, S., Tu, Z.: Text spotting transformers. In: Proceedings of the IEEE/CVF Conference on Computer Vision and Pattern Recognition. pp. 9519–9528 (2022)
48. Zhou, X., Yao, C., Wen, H., Wang, Y., Zhou, S., He, W., Liang, J.: East: an efficient and accurate scene text detector. In: Proceedings of the IEEE conference on Computer Vision and Pattern Recognition. pp. 5551–5560 (2017)
49. Zhu, X., Su, W., Lu, L., Li, B., Wang, X., Dai, J.: Deformable detr: Deformable transformers for end-to-end object detection. *arXiv preprint arXiv:2010.04159* (2020)
50. Zhu, Y., Chen, J., Liang, L., Kuang, Z., Jin, L., Zhang, W.: Fourier contour embedding for arbitrary-shaped text detection. In: Proceedings of the IEEE/CVF conference on computer vision and pattern recognition. pp. 3123–3131 (2021)